Theoretical Study of the HXNY → XNYH (X,Y = O,S) Intramolecular Proton Transfer Reactions

Bárbara Herrera and Alejandro Toro-Labbé*

QTC, Departamento de Quımica Fısica, Facultad de Quımica, Pontificia Universidad Católica de Chile, Casilla 306, Correo 22, Santiago, Chile

Received: August 13, 2003; In Final Form: December 3, 2003

Hartree−Fock and density functional theory calculations are used to study the 1,3-intramolecular proton-transfer reactions in HXNY → XNYH (X,Y = O,S). Energy and a number of reactivity descriptors such as chemical potential, hardness, and electrophilicity index have been studied along the proton-transfer reaction path. It has been found that the profiles of most properties of the 1,3-reordering HXNY → XNYH can be described as a combination of the corresponding profiles of symmetric reactions in which X = Y. A good linear correlation between potential energy and the electrophilicity index in the HONO → ONOH reaction has been found, indicating that any change of these properties during the reaction are well represented in terms of changes in both the electronic chemical potential and molecular hardness.

1. Introduction

In biological systems hydrogen bonds are structural elements that in many cases stabilize the system and are responsible for specific reactivity patterns of both donor and acceptor atoms. Proton transfers (PT) are basic dynamic processes occurring in the core of large aggregate systems such as proteins and nucleic acids; in fact hydrogen bonds stabilize the secondary and tertiary structures of proteins.[1−3] Since the electronic charge migrates in the direction opposite to the proton transfer, PT reactions can be characterized through the response of the system when the electronic density rearranges as the transfer take place. In this context, monitoring global electronic properties such as chemical potential and hardness together with the energy during the process, may give insights on the PT mechanism and should help characterize the effect of the nature of the H-donor and acceptor atoms (O or S) on the energy barriers and electronic structure of PT transition states.

In the framework of density functional theory (DFT), a complete characterization of an *N*-particle system needs only *N* and $v(\vec{r})$, the external potential. The response of the system is measured by the chemical potential (μ) and hardness (η) when *N* is varied for a fixed $v(\vec{r})$.[4−8] μ and η are global properties that together with softness ($S = {}^1/_\eta$) and the electrophilicity index ($\omega = \mu^2/2\eta$) are related to the reactivity of molecular systems and have been quite useful to characterize different kind of systems and processes.[5−12] It has been shown that monitoring the above-mentioned global electronic properties along a reaction coordinate allows one to characterize the electronic reorganization that takes place during the chemical reaction, making it possible to identify specific interactions and propose reaction mechanisms.[10,12−16]

In this work a comparative study of the HXNY → XNYH (X,Y = O,S) series of proton-transfer reactions[17−21] is performed, the aim is 3-fold: (i) identify the specific interactions that are responsible for the stable and transition state species and determine the nature of the potential energy barriers hindering the proton transfer; (ii) classify the asymmetric reaction HSNO → SNOH in terms of reference symmetric processes HONO → ONOH and HSNS → SNSH, and (iii) rationalize the molecular properties of HO−NS and ON−SH in terms of those of the reference species HO−NO and HS−NS. To do so, structural properties, energy, dipole moment, and global reactivity indexes such as chemical potential, hardness, and electrophilicity are studied. On the other hand, the energy and position of the transition state (TS) along a reaction coordinate will be determined by using the Marcus equation[22] and rationalized through the Hammond postulate;[23] these are useful tools that link structural, kinetics and energetic aspects of chemical reactions.[10,12−16]

This paper is organized as follows, in section 2 we review the basic definitions of the electronic properties studied here and define the conceptual frame to characterize the transition states. Section 3 is devoted to the computational details, and in section 4 we present and discuss the results. Section 5 contains our concluding remarks.

2. Theoretical Background

Within the conceptual framework of DFT, chemical potential and hardness of a system of *N* particles with total energy *E* and external potential $v(\vec{r})$ are defined as[5]

$$\mu = \left(\frac{\partial E}{\partial N}\right)_{v(\vec{r})} = -\chi \tag{1}$$

and

$$\eta = \frac{1}{2}\left(\frac{\partial^2 E}{\partial N^2}\right)_{v(\vec{r})} = \frac{1}{2}\left(\frac{\partial \mu}{\partial N}\right)_{v(\vec{r})} \tag{2}$$

In eq 1 χ is the electronegativity.[24−29] Use of the finite difference approximation and Koopmans' theorem leads to the following working expressions for μ and η:

$$\mu \approx -\frac{1}{2}(I + A) = \frac{1}{2}(\epsilon_L + \epsilon_H) \tag{3}$$

and

* Corresponding author. E-mail: atola@puc.cl

10.1021/jp036415z CCC: $27.50
Published on Web 02/14/2004

$$\eta \approx \frac{1}{2}(I - A) = \frac{1}{2}(\epsilon_L - \epsilon_H) \quad (4)$$

where I is the first ionization potential, A is the electron affinity, and ϵ_L and ϵ_H are the energies of the lowest unoccupied molecular orbital (LUMO) and the highest occupied molecular orbital (HOMO), respectively.

Parr et al.[30] defined the electrophilicity index as

$$\omega = \frac{\mu^2}{2\eta} \quad (5)$$

where ω is a measure the stabilization energy of an electron acceptor, at fixed external potential, as it is saturated by a maximum electronic flow from the environment. It is important to stress the fact that the electrophilicity change is determined by changes in μ and η only, ω is therefore a function of μ and η with total differential:

$$d\omega = \left(\frac{\mu}{\eta}\right)d\mu - \frac{1}{2}\left(\frac{\mu}{\eta}\right)^2 d\eta \quad (6)$$

Any variation of ω is therefore linked to variations in μ and η. This link is going to be used to rationalize the variation of ω during the proton-transfer reaction. The maximum electronic charge that the electrophile may accept is $\Delta N_{max} = -\mu/\eta$; using ΔN_{max} in eq 6 applied to finite differences, leads to

$$\Delta\omega = -\left(\Delta N_{max}\Delta\mu + \frac{1}{2}\Delta N_{max}^2\Delta\eta\right) \quad (7)$$

Transition States. PT reactions that are characterized by double-well potential energy profiles present a unique point along the reaction coordinate that defines the transition state (TS), an energy maximum. The energy of the TS can be rationalized through the use of the Marcus equation,[22] in which the energy barrier $\Delta E^{\neq} = [E(\mathrm{TS}) - E(\mathrm{R})]$ is given by

$$\Delta E^{\neq} = \frac{1}{4}K + \frac{1}{2}\Delta E^{\circ} + \frac{(\Delta E^{\circ})^2}{4K} \quad (8)$$

where $K = k_R + k_P$, with $k_{R/P}$ being the force constants associated to reactant and product potential wells and $\Delta E^{\circ} \equiv [E(\mathrm{P}) - E(\mathrm{R})]$ is the reaction energy.[10] Note that for symmetric reactions, since $\Delta E^{\circ} = 0$, the energy barrier $\Delta E^{\neq}$ reduces to $\Delta E_{\circ}^{\neq} = 1/4K$, which is the Marcus intrinsic energy barrier. Differentiating eq 8 with respect to the reaction energy leads to the Brønsted coefficient (β) that following the Leffler postulate[31] characterizes the position of the TS in a reduced reaction coordinate that goes from 0 (at the reactants) to 1 (at the products):[10,32]

$$\beta = \left(\frac{\partial\Delta E^{\neq}}{\partial\Delta E^{\circ}}\right) \Rightarrow \beta = \frac{1}{2} + \frac{\Delta E^{\circ}}{2K} \quad (9)$$

For symmetric reactions $\beta = 1/2$ and $\beta > 1/2$ if $\Delta E^{\circ} > 0$, whereas $\beta < 1/2$ if $\Delta E^{\circ} < 0$. This is in agreement with what is expected from the Hammond postulate,[23] in this context, the Brønsted coefficient is a descriptor of the Hammond postulate.[20,23,32]

3. Computational Details

Three intramolecular proton-transfer reactions involving nitrous acid (HONO) and its sulfur derivatives HSNS, HONS, and HSNO have been characterized by means of theoretical calculations using the Gaussian 98 package.[33] The intrinsic reaction coordinate (IRC)[34,35] is the minimum energy path connecting the transition state to reactants and products. Calculations along the IRC were performed at the HF/6-311G** and B3LYP/6-311G**[36] levels of theory. The reaction path followed by the proton from the donor atom (O or S) to the acceptor atom, passing by the transition state, always lied in the molecular plane. On the other hand, the profiles of energy, chemical potential, hardness, and electrophilicity were obtained through single-point calculations to determine the HOMO and LUMO energies on the previously optimized geometries obtained from the IRC calculation.

TABLE 1: HF//6-311G (first entry) and DFT/B3LYP// 6-311G** (second entry) Bond Distances (Å) and Angles (degrees) of the Stationary Structures for the 1,3-Intramolecular Proton Transfer in HONO, HSNO, and HSNS (for atomic numbering, see Figure 1)**

molecule	(H1)	(12)	(23)	(3H)	(H12)	(123)	(23H)
HONO−(R)	0.932	1.323	1.152	2.081	107.7	113.7	62.0
	0.953	1.324	1.152	2.091	107.9	113.9	62.0
HONO−(TS)	1.261	1.220	1.222	1.261	77.3	105.0	77.5
	1.307	1.258	1.258	1.307	77.4	105.4	77.4
HSNO−(R)	1.334	1.764	1.153	2.461	97.3	116.3	50.3
	1.352	1.927	1.164	2.460	95.5	116.2	51.3
HSNO−(TS)	1.644	1.652	1.210	1.298	63.7	106.2	87.7
	1.665	1.660	1.257	1.372	65.4	107.1	86.1
SNOH−(P)	2.413	1.555	1.300	0.954	50.3	118.5	110.0
	2.425	1.595	1.337	0.985	51.4	117.0	108.5
HSNS−(R)	1.336	1.613	1.506	2.919	108.0	126.3	54.80
	1.336	1.613	1.506	2.918	108.0	126.3	54.82
HSNS−(TS)	1.700	1.597	1.597	1.700	73.3	111.5	73.0
	1.700	1.597	1.597	1.700	73.4	111.5	73.3

4. Results and Discussion

4.1. Geometrical Parameters. When the proton donor and acceptor are atoms having lone pairs, the prediction of equilibrium and transition state geometries are quite difficult because of the spatial disposition of the lone pairs with respect to X···H axis, it appears to be a delicate balance between the factors favoring configurations. Table 1 quotes the HF and B3LYP geometrical parameters of reactants, products, and transition states of the 1,3-intramolecular proton-transfer reactions HXNY(H123) → XNYH(123H) (X,Y = O,S). It should be noted that HF and DFT geometries are quite close to each other, only the transition states present small differences in some bond distances. In addition, the geometrical parameters determined through our calculations are in very good agreement with the available experimental data and also with other theoretical results.[17−19,21]

When comparing the structures of HONO and HSNS we note that the N═O and H−O distances are shorter than N═S and H−S in the disulfur derivative because oxygen has a smaller atomic radius and is a better electron attractor than sulfur. In the asymmetric reaction HSNO → SNOH, it is found that distances and bond angles are quite close to those encountered in symmetrical systems, we observe strong similarities in the geometrical parameters of HSNO and SNOH with appropriate combinations of those of the parent reference molecules HONO and HSNS.

The **TS** for 1,3 intramolecular proton-transfer reactions HXNY → XNYH (X,Y = O,S), were found to be planar pseudopericyclic structures, as illustrated in Figure 1. This is consistent with the 1,3-hydrogen migration in carboxylic acids where also planar transition states were found.[37] The geometry of the transition states provides evidence of π electronic delocalization, an observation that is grounded by the strong

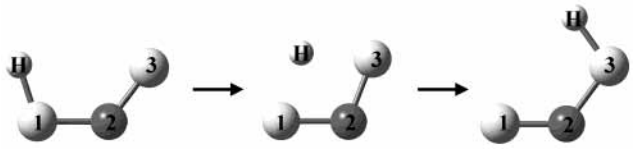

Figure 1. Schematic picture that represents all the H123 → 123H hydrogen transposition reaction considered here.

variations exhibited by the chemical potential along the reaction coordinate (see section 4.4).

4.2. Energy Profiles. In Figures 2a and b are shown the HF and DFT energy profiles for the symmetric PT reactions HXNX → XNXH (X = O,S). The symmetry of the reactions indicates that their transition states are located midway between reactants and products ($\beta = 0.5$). Figure 2c displays the energy profile of the HSNO → SNOH reaction. At both levels of calculation it is found to be an endothermic reaction with barrier heights quite close to that encountered in the HONO → ONOH reaction. This might be indicating that the H···O hydrogen bond determines the nature of the potential barrier. Figure 2c also indicates that the TS is closer to the product ($\beta > 0.5$), in agreement with the Hammond postulate.

In Table 2 are quoted the energetic parameters ($\Delta E°$, $\Delta E^{\neq}$ and $\Delta E^{\neq}_{\circ}$) for the PT reaction at the HF and DFT levels. In all cases the HF barrier is considerably higher than the B3LYP barrier (by about 12−15 kcal/mol). Qualitative analysis of the height and shape of the energy barriers (Figure 2) indicates that some extent of tunneling should be expected; however, it will not be discussed here. With the aim of performing proper comparisons of proton transfer barriers and to identify unambiguously the specific effects that determine the energy barriers, additional calculations of the PT barriers at three new theoretical levels were performed. Post Hartree−Fock perturbation theory (MP2), which is expected to give reasonably good energy barriers, local density approximation (LDA: XαVWN), and generalized gradient approximation (GGA: PW91) have been included with the aim of contrasting the hybrid B3LYP functional within the DFT calculations. In all cases the optimized HF structures of the reference conformations and transition states were used, the results are quoted in Table 2 along with the HF and B3LYP data.

It has been pointed out that DFT methods may fail in estimating potential barriers to proton transfer. This is mainly due to the approximate nature of the functionals that include the so-called self-interaction error.[38] In this context the MP2 results seem to be the most reliable data; they are used as reference when comparing the quality of the different estimation of potential barriers. Table 2 shows that the HF method overestimates the MP2 barriers most probably due to the fact that attractive dispersion interactions are completely missing at the HF level of calculation. Moreover, it has been pointed out that HF often overestimates barrier heights for pericyclic reactions.[39] Dispersion interactions are pure correlation effects and therefore they can only be recovered through correlated levels of theory. On the other hand, the rather crude LDA method (XαVWN) based upon the uniform electron gas approximation, underestimates by far the MP2 barriers. The densities of the systems considered in this work are far from being constant, as required by the LDA approximation, and as a consequence the results obtained with this method are not reliable. The generalized gradient approximation functional PW91, which includes the gradient of the charge density, and the hybrid B3LYP methods lead to more reliable barriers.

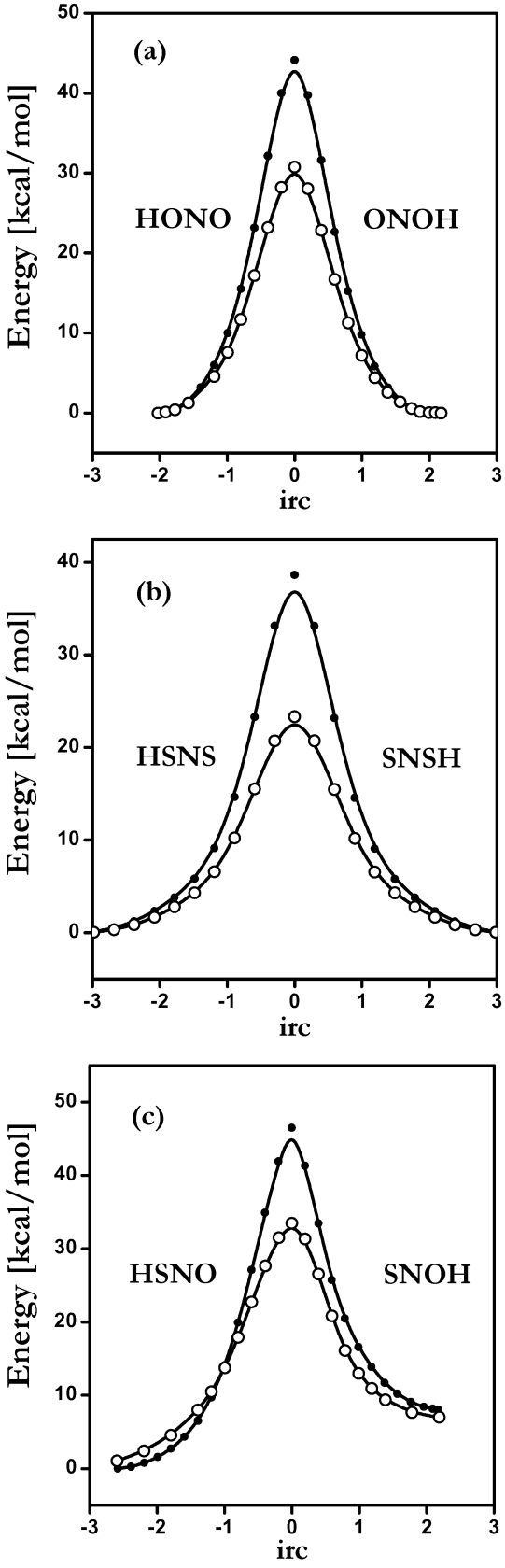

Figure 2. Energy profiles for the 1,3-intramolecular proton transfer in the HXNY series (X,Y = O,S) of reactions at the HF//6-311G** and DFT/B3LYP//6-311G** (open circles) levels of theory. The nuclear movements that define the reaction path are expressed in mass weighted coordinates, thus leading to the unitless IR*C* axis.

The asymmetric HSNO → SNOH reaction was found to be endothermic with $\Delta E°$ fluctuating somewhere between 3 and 8

TABLE 2: Reaction Energy and Potential Barriers Associated with the 1,3-Intramolecular Hydrogen Transfer in the HXNY Series, at Different Levels of Theory

molecule	method	$\Delta E°$	$\Delta E^{\neq}$	$\Delta E^{\neq}_{\circ}$
HONO	MP2	0.00	28.20	
	HF	0.00	44.12	
	B3LYP	0.00	30.75	
	XαVWN	0.00	21.93	
	PW91	0.00	26.14	
HSNO	MP2	3.16	31.09	29.49
	HF	8.00	46.44	42.34
	B3LYP	6.99	33.49	29.89
	XαVWN	3.25	22.67	21.01
	PW91	9.16	30.28	25.49
HSNS	MP2	0.00	18.32	
	HF	0.00	38.63	
	B3LYP	0.00	23.31	
	XαVWN	0.00	14.74	
	PW91	0.00	18.02	

kcal/mol, depending on the level of the calculation. High barriers and positive reaction energies make proton transfer kinetically and thermodynamically unfavorable. Reasons for this can be found in the strong H···O intramolecular hydrogen bond that stabilizes the reactant molecule, whereas in the product molecule (SNOH) the S···H hydrogen bond is weaker, making the whole structure less stable than HSNO.[14] On the other hand, the difference between the strength of the N═O double bond in the reactant and the N═S bond in the product, also helps to explain the above observation. With the aim of characterizing the contribution of the double bond strengths to the energy difference, we have studied the isodesmic reaction $H_2N-SH + HN=O \rightarrow HN=S + H_2N-OH$, obtaining $\Delta E° > 0$ at different levels of calculation. This suggests that the difference between the strength of the N═O and N═S double bonds may also contribute to the endothermicity of the HSNO → SNOH reaction, independent of the hydrogen bonding. Indeed our frequency calculations indicate that the force associated to the N═O stretching vibration is much higher than the force constant associated to the stretching of the N═S bond, a result that is confirmed experimentally.[19,40]

The above observation of the behavior of barrier heights suggests that HSNO and SNOH might be seen as combinations of fragments that behave similarly as in the parent HONO and HSNS molecules. This might be reflected in the energy profiles and in the values of potential barriers. For symmetric reactions $\Delta E° = 0$, the Marcus eq 8 indicates that the intrinsic energetic barrier is given by: $\Delta E^{\neq}_{\circ} = 1/4K$. The value of the intrinsic energy barrier of the HSNO → SNOH reaction has also been calculated from eq 8 with $\Delta E°$ and $\Delta E^{\neq}$ as input data, it is interesting to note that in all calculations $\Delta E^{\neq}_{\circ}$ is found to be quite closer to the $\Delta E^{\neq}_{\circ}$ values of the HONO → ONOH process (in symmetric reactions $\Delta E^{\neq}_{\circ} = \Delta E^{\neq}$), thus common specific interactions determine the height of the barrier. Note that the difference $\Delta E^{\neq}_{\circ} - \Delta E°$ is the intrinsic barrier for the inverse process (SNOH → HSNO). It can be verified that it compares reasonably well with the $\Delta E^{\neq}_{\circ}$ values of the HSNS → SNSH process. This confirms the fact that common specific interactions, in particular hydrogen bonds, featuring in both reference symmetric reactions are the responsible for the nature of the potential barriers in all three PT processes.

It should be noted that HF/6-311G** and B3LYP/6-311G** calculations present trends that are consistent in all three reactions. This observation is also valid for all the properties in which we are interested in this article, so in the remaining analysis we are going to discuss only the HF/6-311G** results but keeping in mind that DFT results follow quite the same trends.

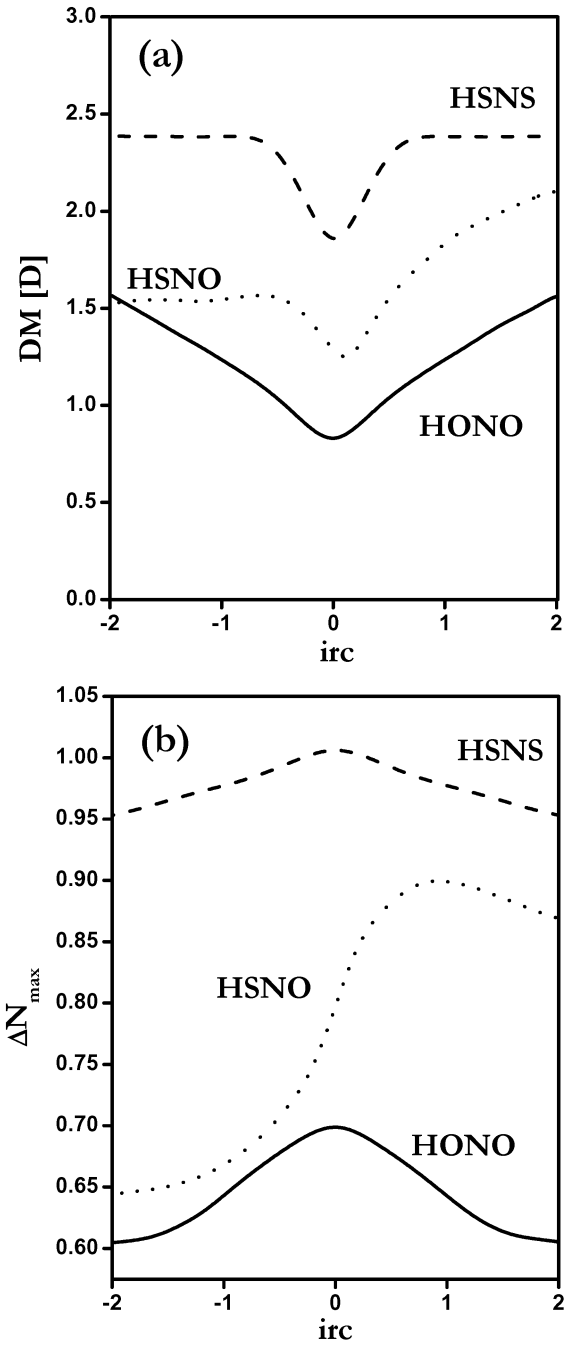

Figure 3. HF//6-311G** dipole moment (DM) and ΔN_{max} profiles along the reaction coordinate for the intramolecular proton transfer in the HXNY series (X,Y = O,S).

4.3. Dipole Moments and Charge Transfer. Figure 3 shows the HF/6-311G** evolution of the dipole moment (DM) and ΔN_{max} for the three PT reactions. All three reactions present opposite extremum values of DM and ΔN_{max} at the TS or near it, opposite trends that indicate that the TSs are mostly characterized by electronic delocalization. This makes the TS structure more electrophilic than the reference conformations.

In the HONO → ONOH reaction, one oxygen atom is acting as donor whereas the second oxygen acts as acceptor of electronic charge during the PT process. The change of the spatial disposition of the lone pairs with respect to the X···H axis produces instantaneous rearrangements of the electronic

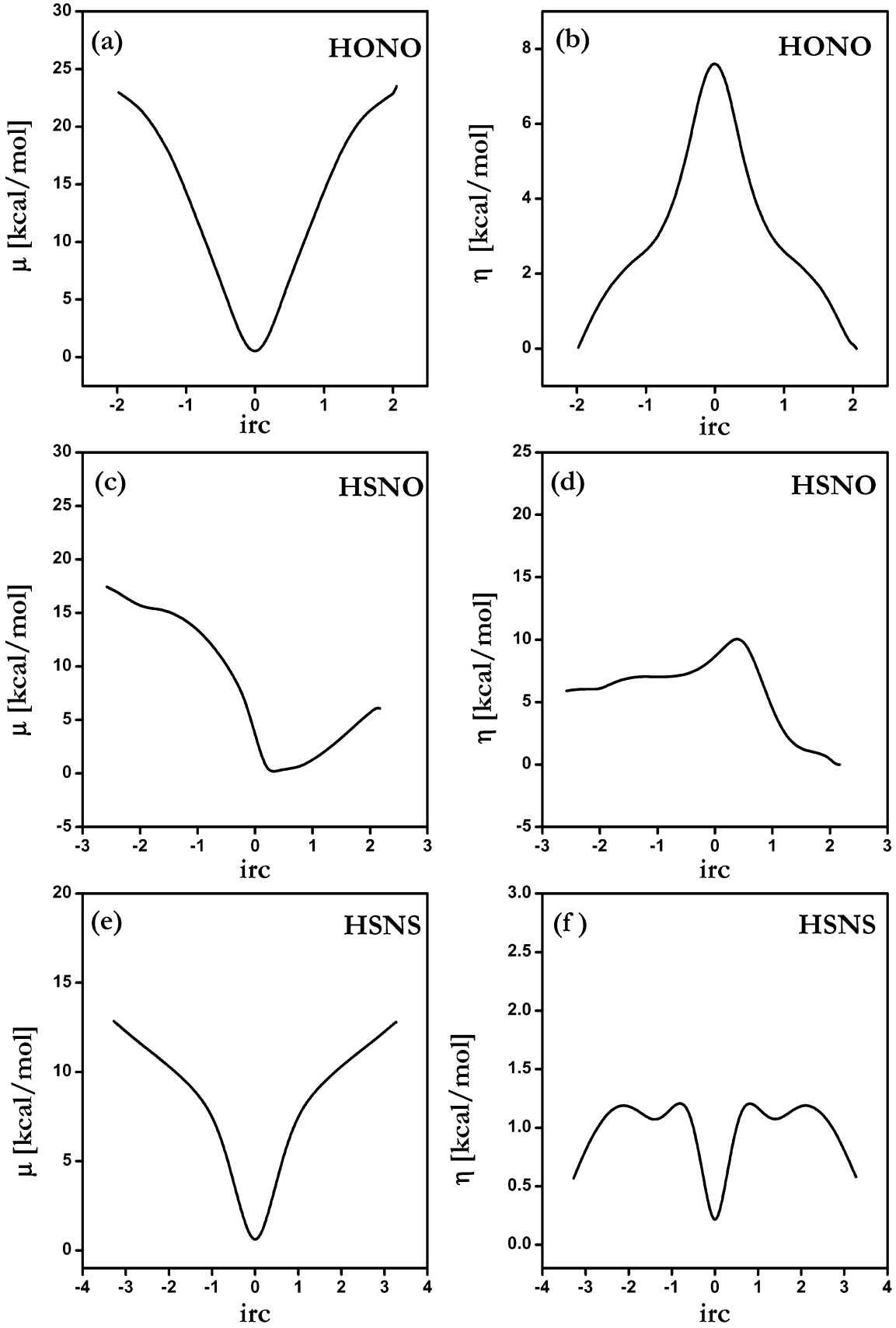

Figure 4. HF//6-311G** profiles of the electronic chemical potential and hardness along the reaction coordinate for the intramolecular proton transfer in the HXNY series (X,Y = O,S).

density, thus leading to quite rapid changes in the dipole moment, to reach a minimum at the symmetric transition state. In addition to the π bond effect that is present in all three systems, in HSNS → SNSH a SNS hyperconjugative interaction

might be favoring a constant value of DM that changes only within the TS region to produce a quite sharp minimum at the TS.

The profiles of ΔN_{max} for the symmetric reactions confirm the above observations, electronic reordering in HONO is stronger than in HSNS. In this latter system the hyperconjugative interaction keeps the ΔN_{max} varying monotonically along the reaction coordinate. These results are consistent with the profiles of chemical potential displayed in Figure 4 where the relative variations of this quantity are indicating that during the PT reaction a reordering of the electronic density is taking place with slightly higher intensity in HONO than in HSNS.

On the other hand, it is interesting to note that the profiles of DM and ΔN_{max} of the asymmetric reaction lie within the interval defined by the profiles of symmetric reactions. In the HSNO → SNOH process the profiles of DM and ΔN_{max} present trends that can be qualitatively associated to those appearing in the reference reactions. Note that in the reactant region, DM is closer in magnitude to that of the HONO reaction but it behaves as the DM in the HSNS system does along the reaction coordinate. This suggests the existence of an SNO hyperconjugative interaction. This situation is inverted at the product region, thus suggesting that the ONS unit cannot bear the hyperconjative interaction.

The above analysis indicates that the DM profile of the HSNO → SNOH reaction can be seen as a combination of the symmetric reaction profiles: when going from R to TS it is qualitatively similar to the corresponding profile of the HSNS reaction; it presents a plateau at the reactant region suggesting that the donor sulfur atom is favoring hyperconjugation that makes the DM to remain constant, and it suddenly decreases to reach a minimum at the TS. From the TS to the products, the DM profiles increase steadily as in the case of the HONO reaction profile, as the reaction moves forward from the TS, the oxygen atom behaves as a nucleophile that concentrates some electronic charge, thus making the dipole moment increase to reach the SNOH final value. Consistent with this analysis, the ΔN_{max} profile shows that at the product region the charge reordering is stronger than at the reactant region.

To close this section it is worth to mention that Mulliken electronic populations on bonds and atoms indicate that the evolution of the electronic populations in donor/acceptor atoms and hydrogen bond regions follow opposite trends: when a proton is transferred the electronic population of the donor atoms increases, whereas that of the acceptor atom decreases indicating that the direction of PT is opposite to the electron transfer.

4.4. Chemical Potential, Hardness, and Electrophilicity. The profiles of μ and η, calculated with the HOMO and LUMO energies using eqs 3 and 4, are displayed in Figure 4. It can be seen that in all the reactions μ changes strongly along the reaction coordinate, the variations of μ[5,8,20,24−27,41−43] indicate that electronic redistribution is taking place along the reaction coordinate and it can be explained in terms of electron transfer from structures with high values of μ to structures with low values of μ. In the present case, Figure 4 shows that the electronic flux is toward the transition state, indicating a considerable degree of electronic delocalization. The π character of the electronic flux may explain the planarity of the transition states. On the other hand, strong variations in μ explain the failure of the principle of maximum hardness (PMH).[44] This principle indicates that when the chemical potential remains reasonably constant, maximum values of η are expected at the energy minimum, whereas the TS should present a minimum value of η.

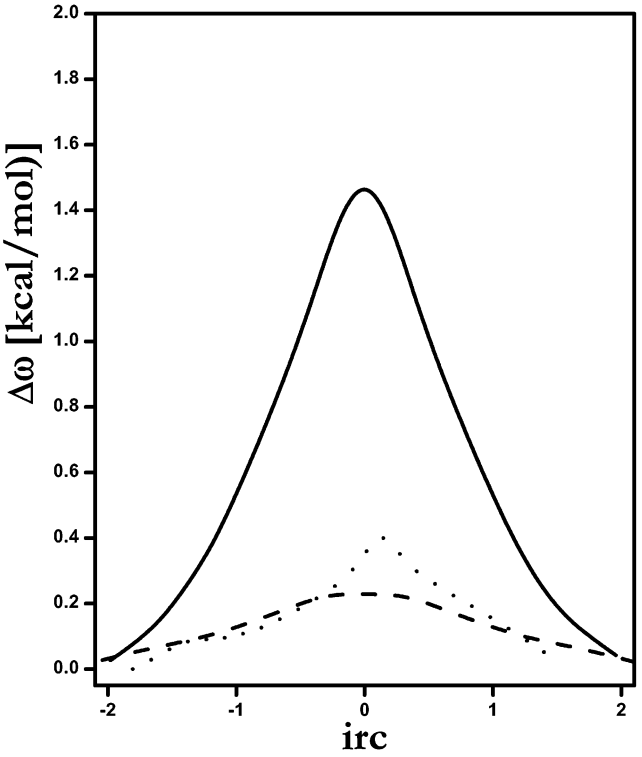

Figure 5. HF//6-311G** profiles of electrophilicity along the reaction coordinate for HONO (full line), HONS (pointed line), and HSNS (dashed line).

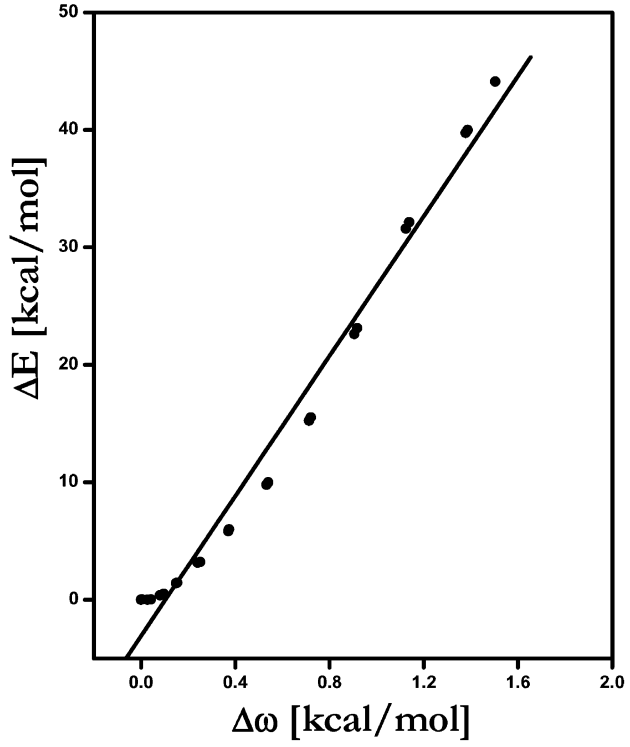

Figure 6. Correlation between HF//6-311G** energy and electrophilicity for the intramolecular HONO → ONOH reaction.

In Figure 5 we present the electrophilicity profiles obtained by using Koopmans values of μ and η. In all cases, the profile of electrophilicity presents quite the same shape as the energy profile, although only the HONO → ONOH reaction presents significant variations of ω along the reaction coordinate. In the HSNO → SNOH and HSNS → SNSH reactions, the stabilization due to saturation of electronic charge coming from the sur-

roundings is not significant and cannot be distinguished from other low energy effects. However for the HONO → ONOH reaction, the variation of ω is significant and its profile is qualitatively similar to that of ΔE shown in Figure 2, this is confirmed by the plot displayed in Figure 6. The $\Delta E-\Delta\omega$ linear relation has been previously encountered[45] and it was shown that this is a necessary condition to express the energy as a function of μ and η only, as they were independent variables.[10]

5. Concluding Remarks

We have characterized the intramolecular proton transfers of the reactions HXNY → XNYH (X,Y = 0,S) through the use of the profiles of energy, dipole moment, chemical potential, hardness, and electrophilicity. It has been found that the HSNO → SNOH reaction can be characterized in terms of combination of the parent symmetric processes in which X = Y = O,S.

The physical nature of the potential energy barrier for the intramolecular proton transfer in the HXNY systems has been identified as being mainly due to the specific hydrogen bonds formed at the reactants and products regions. Systems presenting O···H hydrogen bonds present a higher barrier for proton transfer than those presenting an S···H hydrogen bond. This result was confirmed by the analysis of the trend exhibited by the dipole moment and $\Delta N_{\max}$ profiles of the asymmetric reaction. The evolution of these properties along the reaction coordinate was rationalized in terms of a combination of trends followed by the reference symmetric reactions.

Acknowledgment. This work was supported by FONDECYT through project No. 1020534, and Conicyt by Beca de Apoyo a la Tesis doctoral 2002, B.H. is a Conicyt fellow. We thank an anonymous referee for helpful comments.

References and Notes

(1) Melander, L.; Saunders, W. H. J. *Reaction Rates of Isotopic Molecules*; John Wiley and Sons: New York, 1980.
(2) Jeffrey, G. A.; Saenger, W. *Hidrogen Bonding in Biological Structures*; Springer-Verlag: Berlin, 1991.
(3) Scheiner, S. *Hydrogen Bonding: a Theoretical Perspective*; Oxford University Press: New York, **1997**.
(4) Hohenberg, P.; Kohn, W. *Phys. Rev. B* **1964**, *136*, 834.
(5) Parr, R. G.; Yang, W. *Density Functional Theory of Atoms and Molecules*. Oxford University Press: New Yorik, **1989**.
(6) Parr, R. G.; Donnelly, R. A.; Palke, W. E. *J. Chem. Phys*. **1978**, *68*, 3801.
(7) Parr, R. G.; Pearson, R. G. *J. Am. Chem. Soc*. **1983**, *105*, 7512.
(8) Pearson, R. G. *J. Am. Chem. Soc*. **1985**, *107*, 6801.
(9) Chermette, H. *J. Comput. Chem*. **1999**, *20*, 129.
(10) Toro-Labbé, A. *J. Phys. Chem. A* **1999**, *103*, 4398.
(11) Geerlings, P.; Proft, F. D.; Langenaeker, W. *Chem. Rev*. **2003**, *103*, 1793.
(12) Gutiérrez-Oliva, S.; Jaque, P.; Toro-Labbé, A. *Reviews in Modern Quantum Chemistry*: *A Celebration of the Contributions of Robert G. Parr*; Sen, K. D., Ed.; World Scientific Press: Singapore; p **2002**.
(13) Gutiérrez-Oliva, S.; Letelier, J. R.; Toro-Labbé, A. *Mol. Phys* **1999**, *96*, 61.
(14) Jaque, P.; Toro-Labbé, A. *J. Phys. Chem. A* **2000**, *104*, 995.
(15) Pérez, P.; Toro-Labbé, A. *J. Phys. Chem. A* **2000**, *104*, 1557.
(16) Gutiérrez-Oliva, S.; Jaque, P.; Toro-Labbé, A. *J. Phys. Chem. A* **2000**, *104*, 8955.
(17) Jayakumar, N.; Kolandaivel, P. *Int. J. Quantum Chem*. **2000**, *76*, 648.
(18) Tchir, P. O.; Spratley, R. D. *Can. J. Chem*. **1975**, *53*, 2318.
(19) Nonella, M.; Huber, J. R.; Ha, T. *J. Phys. Chem*. **1987**, *91*, 5203.
(20) M. Solà, Toro-Labbé, A. *J. Phys. Chem. A* **1999**, *103*, 8847.
(21) Jursic, B. S. *Chem. Phys. Lett*. **1999**, *299*, 334.
(22) Marcus, R. A. *Annu. Rev. Phys. Chem*. **1964**, *15*, 155.
(23) Hammond, G. S. *J. Am. Chem. Soc*. **1955**, *77*, 334.
(24) *Hard and Soft Acids and Bases*; Pearson, R. G., Ed.; Dowden, Hutchinson and Ross: Stroudsburg PA, 1973.
(25) Pearson, R. G. Coord. *Chem. Rev*. **1990**, *100*, 403.
(26) Pearson, R. G. *Chemical Hardness*; Oxford, Wiley-VCH: Oxford, Berlin, 1997.
(27) Ayers, P. W.; Parr, R. *J. Am. Chem. Soc*. **2000**, *122*, 2010.
(28) Pauling, L. *The Nature of the Chemical Bond*. Cornell University Press: New York, 1960.
(29) Sen, K. D.; Jorgensen, C. K. *Electronegativity: Structure and Bonding*; Springer-Verlag: Berlin, 1987; vol 66.
(30) Parr, R. G.; Szentpály, L.; Liu, S. *J. Am. Chem. Soc*. **1999**, *121*, 1922.
(31) Leffler, J. E. *Science* **1953**, *117*, 340.
(32) Bulat, F.; Toro-Labbé, A. *J. Phys. Chem. A* **2003**, *107*, 3987.
(33) Frisch, M. J.; Trucks, G. W.; Schlegel, H. B.; Scuseria, G. E.; Robb, M. A.; Cheeseman, J. R.; Zakrzewski, V. G.; Montgomery, J. A., Jr.; Stratmann, R. E.; Burant, J. C.; Dapprich, S.; Millam, J. M.; Daniels, A. D.; Kudin, K. N.; Strain, M. C.; Farkas, O.; Tomasi, J.; Barone, V.; Cossi, M.; Cammi, R.; Mennucci, B.; Pomelli, C.; Adamo, C.; Clifford, S.; Ochterski, J.; Petersson, G. A.; Ayala, P. Y.; Cui, Q.; Morokuma, K.; Malick, D. K.; Rabuck, A. D.; Raghavachari, K.; Foresman, J. B.; Cioslowski, J.; Ortiz, J. V.; Stefanov, B. B.; Liu, G.; Liashenko, A.; Piskorz, P.; Komaromi, I.; Gomperts, R.; Martin, R. L.; Fox, D. J.; Keith, T.; Al-Laham, M. A.; Peng, C. Y.; Nanayakkara, A.; Gonzalez, C.; Challacombe, M.; Gill, P. M. W.; Johnson, B. G.; Chen, W.; Wong, M. W.; Andres, J. L.; Head-Gordon, M.; Replogle, E. S.; Pople, J. A. *Gaussian 98*, revision A. 7; Gaussian, Inc.: Pittsburgh, PA, 1998.
(34) Fukui, K. *Acc. Chem. Res*. **1981**, *14*, 363.
(35) Schlegel, H. *Adv. Chem. Phys*. **1987**, *67*, 250.
(36) Becke, A. D. *J. Chem. Phys*. **1993**, *98*, 5648.
(37) Birney, D. *J. Org. Chem*. **1996**, *61*, 243.
(38) Ciofini, I.; Chermette, H.; Adamo, C. *Chem. Phys. Lett* **2003**, *380*, 12.
(39) Houk, K.; Li, Y.; Evanseck, J. *Angew. Chem., Int. Ed. Engl*. **1992**, *31*, 682.
(40) Carlotti, M.; DiLeonardo, G.; Trombetti, A. *J. Mol. Spectrosc*. **1980**, *84*, 155.
(41) Parr, R. G.; Chattaraj, P. K. *J. Am. Chem. Soc*. **1991**, *113*, 1854.
(42) Chattaraj, P. K. *Proc. Indian Natl. Sci. Acad.-Part A* **1996**, *62*, 513.
(43) Torrent-Sucarrat, M.; Luis, J.; Durán, M.; Solà, M. *J. Am. Chem. Soc*. **2001**, *103*, 7951.
(44) Ayers, P. W.; Parr, R. *J. Am. Chem. Soc*. **2000**, *122*, 2010.
(45) Cadet, J.; Grand, A.; Morell, C.; Letelier, J.; Moncada, J.; Toro-Labbé, A. *J. Phys. Chem. A* **2003**, *107*, 5334.